Transition voltages of vacuum-spaced and molecular junctions with Ag and Pt electrodes

Kunlin Wu, Meilin Bai, Stefano Sanvito, and Shimin Hou

Citation: The Journal of Chemical Physics **141**, 014707 (2014); doi: 10.1063/1.4886378
View online: http://dx.doi.org/10.1063/1.4886378
View Table of Contents: http://scitation.aip.org/content/aip/journal/jcp/141/1?ver=pdfcov
Published by the AIP Publishing

Transition voltages of vacuum-spaced and molecular junctions with Ag and Pt electrodes

Kunlin Wu,[1] Meilin Bai,[1] Stefano Sanvito,[2] and Shimin Hou[1,a)]
[1]*Key Laboratory for the Physics and Chemistry of Nanodevices, Department of Electronics, Peking University, Beijing 100871, China*
[2]*School of Physics, AMBER and CRANN Institute, Trinity College, Dublin 2, Ireland*

(Received 23 April 2014; accepted 20 June 2014; published online 7 July 2014)

The transition voltage of vacuum-spaced and molecular junctions constructed with Ag and Pt electrodes is investigated by non-equilibrium Green's function formalism combined with density functional theory. Our calculations show that, similarly to the case of Au-vacuum-Au previously studied, the transition voltages of Ag and Pt metal-vacuum-metal junctions with atomic protrusions on the electrode surface are determined by the local density of states of the p-type atomic orbitals of the protrusion. Since the energy position of the Pt 6*p* atomic orbitals is higher than that of the 5*p*/6*p* of Ag and Au, the transition voltage of Pt-vacuum-Pt junctions is larger than that of both Ag-vacuum-Ag and Au-vacuum-Au junctions. When one moves to analyzing asymmetric molecular junctions constructed with biphenyl thiol as central molecule, then the transition voltage is found to depend on the specific bonding site for the sulfur atom in the thiol group. In particular agreement with experiments, where the largest transition voltage is found for Ag and the smallest for Pt, is obtained when one assumes S binding at the hollow-bridge site on the Ag/Au(111) surface and at the adatom site on the Pt(111) one. This demonstrates the critical role played by the linker-electrode binding geometry in determining the transition voltage of devices made of conjugated thiol molecules.
 [http://dx.doi.org/10.1063/1.4886378]

I. INTRODUCTION

Molecular electronic devices, in which single molecules are used as the functional active element, are believed to have the potential of continuing electronic devices miniaturization beyond the limits of the conventional silicon-based technology.[1,2] The current-voltage, I-V, characteristics of molecular devices is dominated by the quantum nature of the molecule, the band structure of the electrodes, and the electronic coupling at the molecule-electrode interface. Therefore, the electrodes' composition and their shape play an important role in the electronic transport properties of molecular devices, and in particular they determine the alignment of various molecular levels relative to the electrode Fermi energy, E_F. Recently Beebe *et al.* introduced transition voltage spectroscopy (TVS) as a measure of the energy alignment between the frontier molecular orbitals and the electrodes' E_F.[3,4] Due to its simplicity and sensitivity, TVS is becoming an increasingly popular spectroscopic tool for molecular devices[5–20] and has been even extended to characterize vacuum-spaced junctions such as Au/vacuum/Au.[21] It has been shown that the transition voltage of an oligo(phenylene ethynylene) molecule attached with a thiol(isocyanide) linker group to four different metal electrodes, Ag, Pd, Au, and Pt, decreases (increases) as the electrode work function gets larger, and that the change of the measured transition voltage is smaller than the corresponding change in work function.[4] These experimental findings were explained with a simple barrier picture, and the transition voltages were related to the effective barrier height determined by the electrode E_F and the closest molecular orbital. However, it has been demonstrated that models for tunneling over an energy barrier are not appropriate for molecular junctions,[22] even not for Au/vacuum/Au junctions.[23] In contrast, the coherent Landauer transport formalism appears more appropriate for the problem at hand, with the transition voltage being related to the applied bias voltage, which promotes a significant spectral weight of the transmission function into the bias window.[24] By employing the non-equilibrium Green's function formalism combined with density functional theory (i.e., the NEGF+DFT approach),[25–34] we have shown that the calculated transition voltages of three different asymmetric Au/poly(phenylene) thiol/Au molecular junctions can be in quantitative agreement with the experimental values at positive polarity.[35] Thus, it is highly desirable to carry out studies beyond the tunneling barrier model in order to investigate the effects of the electrodes' composition and their shape on the transition voltages of molecular junctions. These will enable TVS to become a widely used tool for understanding charge transport mechanism of molecular electronic devices.

These issues are investigated theoretically by calculating the electronic transport properties of vacuum-spaced and molecular junctions constructed with Ag and Pt electrodes. Although not as popular as gold, Ag and Pt are often employed as electrode materials for constructing molecular junctions.[36–44] Silver and gold are both noble metals whose density of states (DOS) around E_F is dominated by s-type

a)Author to whom correspondence should be addressed. Electronic mail: smhou@pku.edu.cn

orbitals, while platinum is a transition metal having a DOS with strong d-character around the Fermi level. Thus, it is interesting to establish whether the electronic transport properties of vacuum-spaced junctions constructed with Ag and Au electrodes are significantly different from those made with Pt. At the same time these studies on metal-vacuum-metal junctions can provide an important reference for molecular devices made with the same metal electrodes.

In order to make a comparison with our previous results for Au/poly(phenylene) thiol/Au junctions,[35] here biphenyl thiol is chosen as the central molecule. Similarly to the case of gold, chemisorption always occurs when organosulfur compounds adsorb on Ag and Pt surfaces.[45,46] Using the NEGF+DFT approach, our calculations show that the transition voltage of metal-vacuum-metal junctions with atomically sharp electrodes is not directly related to the vacuum barrier shape but is mainly determined by the local density of states (LDOS) of the p-type atomic orbitals of the metal apex atom. Since the position of the LDOS peak contributed by the 5*p* atomic orbitals of the Ag apex atom on the Ag(111) surface is almost the same as that contributed by the 6*p* atomic orbitals of the Au apex atom on the Au(111) surface, the transition voltage of Ag-vacuum-Ag junctions is very close to that of Au-vacuum-Au ones. In contrast, the LDOS of the 6*p* atomic orbitals of the Pt apex atom on the Pt(111) surface is higher in energy with respect of the case of Ag and Au. As a consequence Pt-vacuum-Pt junctions have a much larger transition voltage than Ag-vacuum-Ag (or Au-vacuum-Au) ones. For asymmetric biphenyl thiol molecular junctions, the transition voltage at positive polarity is related to the highest occupied molecular orbital (HOMO), since the HOMO-dominated transmission peak is closer to the electrodes' Fermi level than that attributed by the lowest unoccupied molecular orbital (LUMO). Moreover, the position of the HOMO-dominated transmission peak is determined not only by the electrode material but also by the details of the bonding configuration of the thiolate group. When the sulfur atom binds at the hollow-bridge site of the Au(111) or the Ag(111) surface and at the adatom site of the Pt(111) one, Ag-biphenyl thiol-Ag junctions have the highest transition voltage while Pt-biphenyl thiol-Pt junctions have the lowest, in agreement with the experimental trend for conjugated thiol molecules.[4]

II. CALCULATION METHOD

In this work we use the SIESTA code[47] to compute the atomic structure of both vacuum-spaced and molecular junctions with Ag and Pt electrodes and the quantum transport code SMEAGOL[32–34] to study their electronic transport properties. SIESTA is an efficient DFT package, which makes use of improved Troullier–Martins pseudopotentials for describing the atomic cores and adopts a finite-range numerical orbital basis set to expand the wave functions of the valence electrons.[47,48] While a double-zeta plus polarization (DZP) basis set is used for H, C, and S, two different types of basis functions are used for Ag and Pt, respectively in the bulk and at the surface. In more detail, a double-zeta basis set augmented with polarization and diffuse functions (DZP+diffuse) is used for the surface Ag and Pt atoms, while a single-zeta plus polarization (SZP) basis is used for the bulk. This allows us to keep a balance between the efficiency and the required accuracy of the simulations.[49,50] The exchange-correlation functional is at the level of the generalized gradient approximation (GGA) within the Perdew-Burke-Ernzerhof (PBE) formulation.[51] Geometry optimization is performed by standard conjugate gradient relaxation until the atomic forces are smaller than 0.03 eV $Å^{-1}$.

SMEAGOL is a practical implementation of the NEGF+DFT approach, which employs SIESTA as the DFT platform.[32–34] We use an equivalent cutoff of 200.0 Ryd for the real space grid. The charge density is integrated over 36 energy points along the semi-circle, 36 along the line in the complex plane, 240 along the real axis, while 36 poles are used for the Fermi function (the electronic temperature is 25 meV). And the convergence criterion is set to be 1×10^{-4} for the density matrix. We always consider periodic boundary conditions in the plane transverse to the transport. The unit cell of the extended molecule comprises ten Ag(111) or Pt(111) atomic layers with a (3×3) in plane supercell and one biphenyl thiol molecule for molecular junctions. The *I–V* curve of the junction is calculated as

$$I = \frac{2e}{h}\int_{-\infty}^{+\infty} T(V, E)[f(E-\mu_L) - f(E-\mu_R)]dE, \quad (1)$$

where *T (V, E)* is the bias-dependent transmission coefficient of the junction, *f (E)* is the Fermi function, $\mu_{L/R} = E_F \pm eV/2$ is the local Fermi level of the left/right electrode. The transition voltage is obtained from the minimum appearing in the Fowler-Nordheim (F-N) plot of the *I-V* data, i.e., a plot of $\ln(I/V^2)$ against 1/V. Then, the total transmission coefficient *T(V, E)* of the junction is evaluated as

$$T(V, E) = \frac{1}{\Omega_{2DBZ}}\int_{2DBZ} T(\vec{k}; V, E)d\vec{k}, \quad (2)$$

where Ω_{2DBZ} is the area of the two-dimensional Brillouin zone (2DBZ) in the transverse directions. The *k*-dependent transmission coefficient $T(\vec{k}; V, E)$is obtained as

$$T(\vec{k}; V, E) = Tr[\Gamma_L G_M^R \Gamma_R G_M^{R+}], \quad (3)$$

where G_M^R is the retarded Green's function matrix of the extended molecule and Γ_L (Γ_R) is the broadening function matrix describing the interaction of the extended molecule with the left-hand (right-hand) side electrode. Here, we calculate the transmission coefficient by sampling 4×4 k-points in the transverse 2DBZ.

III. RESULTS AND DISCUSSION

A. TVS of vacuum-spaced junctions with Ag and Pt electrodes

We start our analysis from the investigation of the electronic transport properties of the Ag-vacuum-Ag junction. Considering that in a typical break junction a single-atom contact is always formed between the two silver electrodes before the junction rupture,[38] two symmetric Ag-vacuum-Ag junction models are constructed. In these either one Ag adatom or

a Ag cluster with four atoms arranged in a pyramid configuration is attached to the Ag(111) surfaces [see Figures 1(a) and 1(g)]. For the sake of brevity, these two junction models are denoted as Ag-Junction-Adatom and Ag-Junction-Pyramid. Figures 1(b) and 1(h) present the equilibrium transmission spectra of these two junctions in which the distances between the two apex atoms are respectively set to 6.05 Å and 5.99 Å. As one can see, the transmission below the Fermi level is very small since the charge density associated to the 4*d* atomic orbitals of the apex silver atoms decays very quickly into the vacuum. Around E_F the 5*s* atomic orbital of the apex silver atom dominates the LDOS, thus the transmission as a function of energy is rather smooth. In contrast, a few transmission peaks appear above the Fermi level. These originate mainly from the 5*p* atomic orbitals of the apex atoms due to their relatively slow decay in vacuum. Since the interaction between the atom at the apex of the pyramid and the Ag(111) surface is much weaker than that between the Ag adatom and the Ag(111) surface, the transmission peak in Ag-Junction-Pyramid is much sharper than that in Ag-Junction-Adatom and also localized at higher energies. At the Fermi level the transmission coefficients of Ag-Junction-Adatom and Ag-Junction-Pyramid are calculated to be 1.1×10^{-2} and 1.8×10^{-2}, respectively.

When a bias voltage is applied, the *I-V* curve shows a transition from a linear dependence at low voltage to a pronounced nonlinear behavior at high voltage. As a result, a well-defined minimum appears in the F-N plots of these two junctions [see Figures 1(e) and 1(k)], and the transition voltages are respectively determined to be 1.4 V and 2.1 V for Ag-Junction-Adatom and Ag-Junction-Pyramid. These values are very close to those calculated for the Au-vacuum-Au junctions with the same electrode shape[48] and the difference is smaller than 0.1 V. Since the work function of the Ag(111) surface (4.74 eV) is almost 0.6 eV smaller than that of the Au(111) one (5.31 eV),[52] the similarity in the transition voltage between the two junctions demonstrates that the transition voltage of vacuum-spaced junctions with atomic protrusions is not simply directly related to the vacuum barrier height.

A deeper insight into the transition voltages of these two junctions can be obtained by plotting their bias-dependent transmission spectra [Figures 1(f) and 1(l)]. Clearly, as the bias voltage increases the transmission peak above the Fermi level is broadened while its intensity simultaneously decreases. Furthermore, its rising edge moves towards the electrodes' Fermi level continuously and the current through the junction increases rapidly as soon as the peak enters the bias window defined by the two electrodes' local chemical potentials. At such bias an inflection appears in the F-N plot. This process is more pronounced in Ag-Junction-Pyramid due to the sharpness of its transmission peak. Considering that the transmission peak is closely related to the LDOS peak contributed by the 5*p* atomic orbitals of the apex, the transition voltage of these Ag-vacuum-Ag junctions with atomically sharp electrodes is determined by the LDOS of the apex silver atom on the electrode surface and its value roughly equals the rising edge of the LDOS peak contributed by the 5*p* atomic orbitals of the apex located on the electrode shifting downwards in energy. This analysis is supported by the dependence of the calculated transition voltage on the electrode distance and the bias polarity. For both Ag-Junction-adatom and Ag-Junction-pyramid, the transition voltage shows a weak distance-dependence. For example, when the electrode distance in Ag-Junction-Adatom is increased from 5.20 Å to 6.05 Å and finally to 7.05 Å, the transition voltage changes from 1.5 V to 1.4 V to 1.3 V. This can be understood as follows. When the electrode distance is large enough for the transition voltage to be detected, the interaction between the two silver electrodes is rather weak and thus the LDOS of the apex silver atom is mainly determined by its local atomic

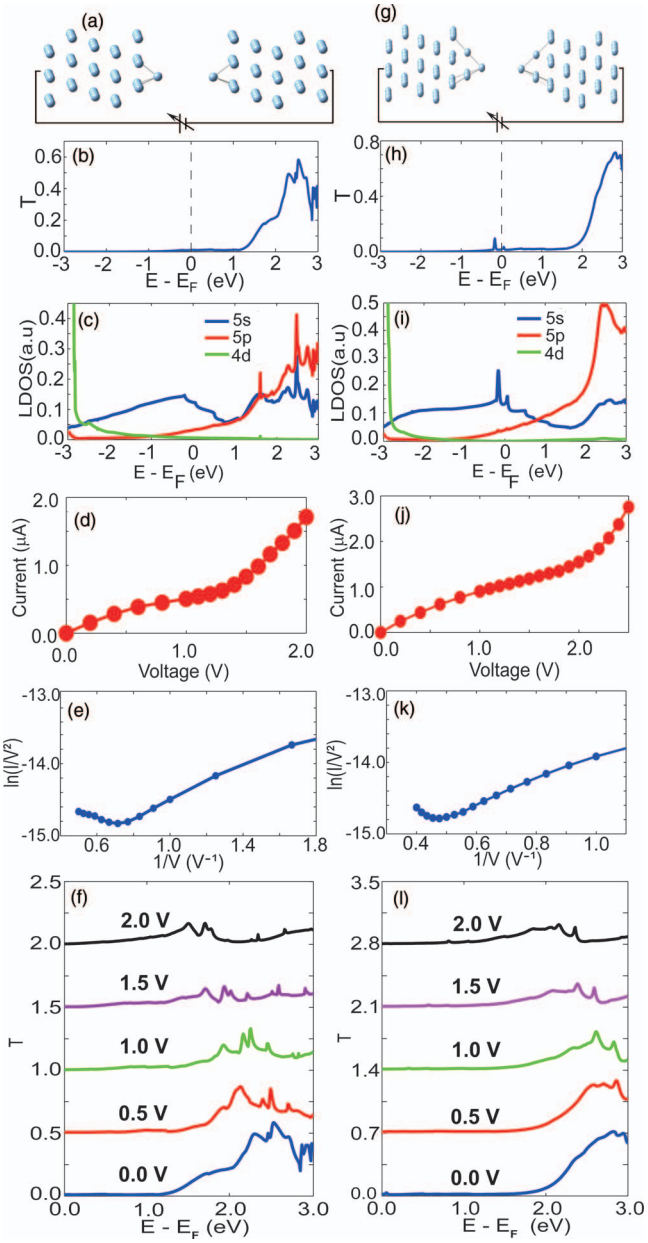

FIG. 1. Transport properties and electronic structure of Ag-Junction-Adatom and Ag-Junction-Pyramid. In the panels on the left we show: optimized atomic structure (a), zero-bias transmission spectrum (b), LDOS corresponding to the Ag adatom (c), I-V curve (d), F-N plot (e), and the bias-dependent transmission spectra (f) of Ag-Junction-Adatom. For Ag-Junction-Pyramid the same quantities are plotted in the right-hand side panels (g)–(l). The various plot in panel (f) and (l) are displaced vertically for clarity.

structure, leading to the weak distance-dependence of the transition voltage.

Due to their symmetric atomic structure, the LDOS of the two apex silver atoms in both Ag-Junction-Adatom and Ag-Junction-pyramid are identical and thus their transition voltage does not depend on the bias polarity. However, the situation changes dramatically in asymmetric Ag-vacuum-Ag junctions. For example, one asymmetric Ag-vacuum-Ag junction is constructed with the surfaces of the two silver electrodes decorated respectively with a silver adatom at one side and a four-atom silver cluster in the pyramid configuration at the other, and with the distance between the two apex silver atoms being set to 6.08 Å (Fig. S1 in the supplementary material).[53] Since the LDOS of the adatom and the pyramid apex are drastically different [see Figures 1(c) and 1(i)], one can expect that the transition voltages of this asymmetric Ag-vacuum-Ag junction will depend strongly on the bias polarity. This is indeed the case. When a positive voltage is applied to the electrode containing the silver adatom, the current through the junction increases rapidly following the increase of the applied bias and the transition voltage is determined to be 1.4 V, i.e., it is the same as Ag-Junction-Adatom with the same electrode distance. In contrast, when the bias polarity is reversed, the increase of the current becomes much slower and the transition voltage increases to 2.2 V, which is only 0.1 V larger than that of the Ag-Junction-Pyramid configuration with the same electrode distance. Such picture is completely consistent with the fact that the LDOS peak contributed by the 5*p* atomic orbitals of the silver adatom is much lower in energy than that of the silver atom at the pyramid apex.

The transition voltages of the symmetric and asymmetric Ag-vacuum-Ag junctions not only have a value very close to that of their Au counterparts, but also show the same dependence on the electrode distance and the bias polarity. This can also be explained by the fact that the transition voltage is determined by the LDOS of the apex atom on the electrode surface. Due to the large relativistic effects, the electronic structure of bulk gold is significantly different from that of bulk silver, especially when considering the positions of the *d*-bands relative to the Fermi level.[54] In the Au/Ag-vacuum-Au/Ag junctions with atomically sharp electrodes investigated here, the LDOS contributed by the 4*d* atomic orbitals of the apex silver atom is also far below the Fermi level compared with that contributed by the 5*d* atomic orbitals of the apex gold atom.[50] However, the positions of the LDOS peaks contributed by the 5*p* orbitals of the apex silver atom are almost the same as those contributed by the 6*p* orbitals of the apex gold atom. Thus, the transition voltage of the various Ag-vacuum-Ag junctions has the same properties as that of the corresponding Au-vacuum-Au ones.

Let us now move our attention to the electronic transport properties of Pt-vacuum-Pt junctions. Taking the same geometric structure as that of Ag-Junction-Adatom, a symmetric Pt-vacuum-Pt junction model is constructed with one Pt adatom attached to each electrode surface [see the inset of Fig. 2(a)]. This is termed Pt-Junction-Adatom for short. Fig. 2(a) shows the equilibrium transmission spectrum of such junction when the distance between the two Pt adatoms is set to be 5.81 Å. Similarly to that of Ag-Junction-Adatom

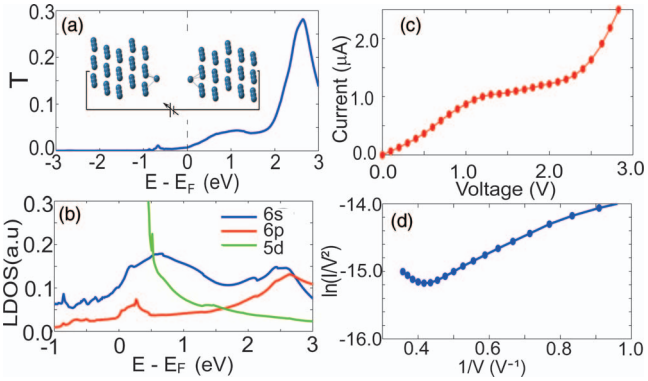

FIG. 2. Transport properties of the Pt-Junction-Adatom: zero-bias transmission spectrum (a), LDOS corresponding to the platinum adatom (b), the I-V curve (c), and the F-N plot (d). The insert of panel (a) shows the optimized atomic structure.

(Fig. 1(b)), the transmission of Pt-Junction-Adatom below the Fermi level is very small, because the 5*d* atomic orbitals of the Pt adatom dominate the LDOS in this energy range and their wave functions decay rapidly into the vacuum. However, above E_F the transmission of the Pt-Junction-Adatom increases more slowly than that of Ag-Junction-Adatom and one transmission peak appears at 2.64 eV. This can be traced to the different behavior of the LDOS contributed by the *p*-type atomic orbitals of the adatom. For the Ag adatom, its 5*p* atomic orbitals dominate the LDOS from about 1.0 eV above the Fermi level. In contrast, the same happens for the Pt adatom only starting from about 2.0 eV above E_F. Correspondingly, the transition in the *I*-*V* curve from a linear dependence to a pronounced nonlinear behavior only occurs at about 2.0 V for the Pt-Junction-Adatom. Thus, the associated transition voltage is now 2.3 V, almost 1 V larger than that of Au/Ag-vacuum-Au/Ag junctions with the same electrode shape. Also for the Pt-Junction-Adatom the distance dependence of the transition voltage is weak. For example, when the distance between the two Pt adatoms is increased from 5.81 Å to 6.81 Å, the transition voltage does not change and remains at 2.3 V.

If each Pt adatom in Pt-Junction-Adatom is replaced by a Pt cluster with four atoms arranged in a pyramid configuration (Fig. S2 in the supplementary material), the transmission peak above the Fermi level is further shifted upwards in energy. This is the consequence of the movement of the LDOS peak contributed by the 6*p* atomic orbitals of the apex Pt atom to higher energies, as a result of the weakened interaction with the Pt(111) surface. Thus, we can expect the transition voltage of this Pt-vacuum-Pt junction to be larger than that of Pt-Junction-Adatom. However, due to numerical instabilities at such high bias voltages, we could not calculate the exact value of that transition voltage.

B. TVS of molecular junctions with Ag and Pt electrodes

Now we move to investigate the electronic transport properties of molecular junctions constructed with Ag and Pt electrodes. First, we connect the biphenyl thiol molecule to

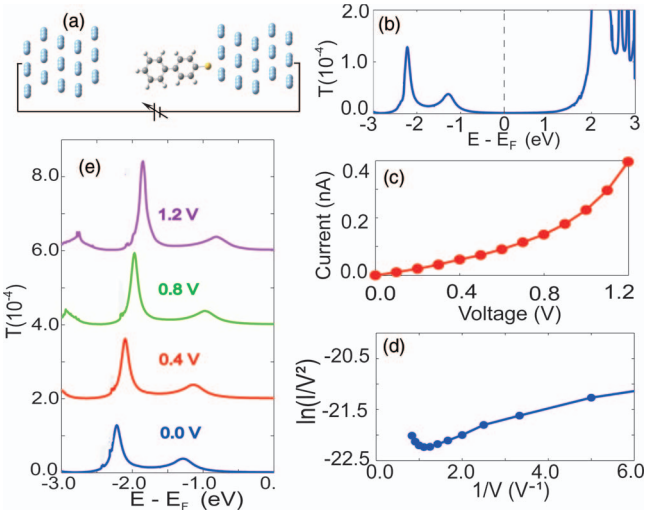

FIG. 3. Transport properties of a Ag-biphenyl thiol-Ag junction constructed with two atomically flat electrode surfaces: the optimized atomic structure (a), the zero-bias transmission spectrum (b), the I-V curve (c), the F-N plot (d), and the bias-dependent transmission spectra (e). The transmission spectra except for $V = 0$ are vertically offset for clarity.

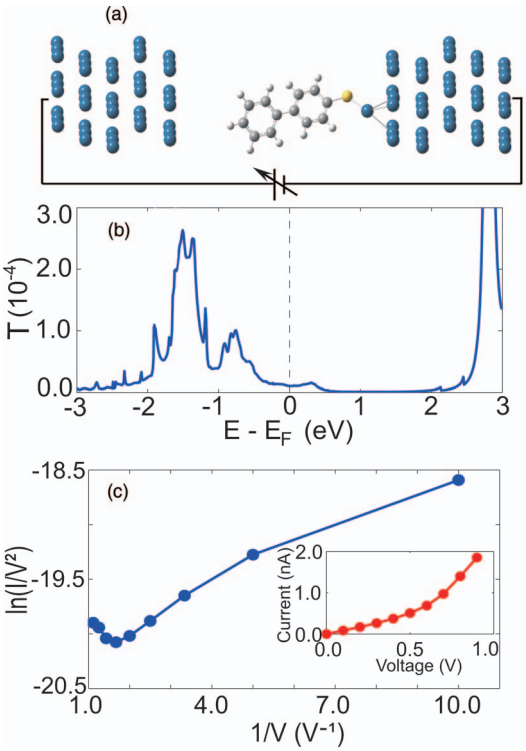

FIG. 4. Transport properties of a Pt-biphenyl thiol-Pt junction in which the sulfur atom binds at the adatom site and the phenyl ring directly faces the Pt(111) surface: the optimized atomic structure (a), the zero-bias transmission spectrum (b), and the F-N plot (c). The inset in panel (c) shows the *I-V* curve on a linear scale.

two silver electrodes with an atomically flat Ag(111) surface [see Fig. 3(a)]. After optimization, the sulfur atom is found to be located between the bridge and the hollow site with an average Ag-S bond length of 2.61 Å and with the shortest Ag-H distance at the Ag-phenyl interface being 5.23 Å. The corresponding equilibrium transmission spectrum is given in Fig. 3(b). As we can see, around the Fermi level three broad transmission peaks appear respectively at −2.22 eV, −1.28 eV, and 2.18 eV. Eigenchannel analysis reveals that these three transmission peaks originate respectively from the biphenyl thiol HOMO − 1, HOMO, and LUMO (Fig. S3 in the supplementary material).[55,56] When compared with the Au-biphenyl thiol-Au junction with the same molecule-electrode interfaces,[35] the positions of these transmission peaks turn out to be shifted to lower energies. For example, the replacement of gold electrodes with silver ones moves the HOMO-dominated transmission peak from −0.96 eV down to −1.28 eV.

Since the HOMO-dominated transmission peak is closer to the Fermi level than that contributed by the LUMO and since the transmission at the peak (3.8×10^{-5}) is also much larger than that at the Fermi level (1.4×10^{-6}), one can expect that the current through the junction will increase rapidly after the tail of the HOMO enters the bias window. This is realized by applying a positive bias voltage to the silver electrode connected to the biphenyl thiol molecule through the Ag-phenyl interface. As shown in Fig. 3(e), when the bias voltage increases the HOMO transmission peak moves almost rigidly to high energies. As soon as the HOMO-dominated transmission peak enters the bias window, the current through the Ag-biphenyl thiol-Ag junction increases nonlinearly and thus a well-defined minimum appears in the F-N plot, giving a transition voltage of 0.9 V [Fig. 3(d)]. The calculated transition voltage is insensitive to the variations of the distance between the Ag electrode and the biphenyl thiol molecule, which is defined by the shortest Ag-H distance at the Ag-phenyl interface. For example, when the Ag-H distance is elongated to 6.00 Å or is shortened to 3.88 Å, the transition voltage remains at 0.9 V. This result is not surprising. The coupling between the biphenyl thiol molecule and the Ag electrode at the Ag-phenyl interface is much weaker than that at the Ag-S contact, thus varying the Ag-H distance does change the tunneling barrier width at the Ag-phenyl interface but affects marginally the alignment of the biphenyl thiol molecular orbitals relative to the electrode Fermi level. The calculated transition voltages of the Ag-biphenyl thiol-Ag junctions are always larger than those of the Au-biphenyl thiol-Au junctions with the same molecule-electrode interfaces, in good agreement with the experimental results reported for conjugated thiol molecules.[4]

Next we extend our studies to asymmetric biphenyl thiol molecular junctions made of Pt electrodes. As shown in Fig. 4(a), at one side of the Pt-biphenyl thiol-Pt junction the sulfur atom is assumed to bind at the adatom site of the Pt(111) surface and the Pt-S bond length is optimized to be 2.24 Å. At the other side, the phenyl ring directly faces the atomically flat Pt(111) surface and the shortest Pt-H distance is calculated to 5.09 Å. Fig. 4(b) presents the equilibrium transmission spectrum of this Pt-biphenyl thiol-Pt junction model, in which the transmission peaks located at −1.37 eV, −0.75 eV, and 2.80 eV are respectively contributed by the HOMO − 1, HOMO, and LUMO of the biphenyl thiol molecule. Since the HOMO-dominated transmission peak is very close to the Fermi level, the current through the junction increases rapidly as the bias voltage is increased [see

Fig. 4(c)]. Correspondingly, the transition voltage is only 0.6 V, the smallest among all molecular junctions constructed with these three types of electrode materials (Ag, Au, and Pt). Varying the Pt-H distance does not affect the calculated transition voltage too much. For example, the transition voltage remains at 0.6 V when the Pt-H distance is elongated to 6.00 Å or shortened to 3.84 Å.

It should be noted that the transition voltage of the Pt-biphenyl thiol-Pt junction depends strongly on the bonding configuration of the Pt-S contact. For example, when the sulfur atom binds at the hollow site of the Pt(111) surface, the HOMO-dominated transmission peak is shifted down to −1.35 eV (Fig. S4 in the supplementary material). As a result, the current increases rather slowly and no minimum appears in the F-N plot up to voltages as large as 1.0 V. Therefore, besides the electrode material the binding configuration of the sulfur atom on the electrode surface is another vital factor determining the transition voltage.

IV. CONCLUSION

We have investigated the transition voltage of vacuum-spaced and molecular junctions with Ag and Pt electrodes using the NEGF+DFT approach, and found that the transition voltages of Ag-vacuum-Ag junctions with atomically sharp electrodes are very similar to those of Au-vacuum-Au junctions, although the work function of the Ag(111) surface is significantly smaller than that of the Au(111) one. This originates from the fact that the transition voltage of metal-vacuum-metal junctions with atomic protrusions on the electrode surface is determined by the LDOS peak contributed by the p-type atomic orbitals of the metal apex atom rather than by the vacuum barrier shape and that the position of the LDOS peak contributed by the 5*p* atomic orbitals of the Ag apex atom is similar to that contributed by the 6*p* atomic orbitals of the Au apex atom. Compared with Ag-vacuum-Ag and Au-vacuum-Au junctions, the LDOS peak contributed by the 6*p* atomic orbitals of the Pt apex atom is positioned at a higher energy thus the transition voltages of Pt-vacuum-Pt junctions have a much larger value. For the asymmetric biphenyl thiol molecular junctions with Ag and Pt electrodes, the transition voltage at positive polarity is mainly determined by the HOMO-dominated transmission peak. Because both the electrode material and the binding site of the sulfur atom affect the alignment of the biphenyl thiol molecular orbitals relative to the electrode Fermi level, the calculated transition voltages are found to be in descending order for the Ag, Au, and Pt electrodes when the sulfur atom binds at the hollow-bridge site of the Ag/Au(111) surface and the adatom site of the Pt(111) surface, which agrees well with the experimental trend of the transition voltages for conjugated thiol molecules. It should be pointed out that this result is obtained by using the PBE GGA functional. Although PBE GGA can describe well the band structure of metals, it usually overestimates the HOMO level and underestimates the HOMO-LUMO gap of molecules. Therefore, further investigations on the effects of DFT functionals on the calculated transition voltage will be carried out in the future.

ACKNOWLEDGMENTS

This project was supported by the National Natural Science Foundation of China (Grant No. 61321001) and the MOST of China (Grant Nos. 2011CB933001 and 2013CB933404). S.S. thanks additional funding support from the European Research Council (QUEST project), by KAUST (FIC/2010/08), and by AMBER.

[1] N. J. Tao, Nat. Nanotechnol. **1**, 173 (2006).
[2] H. Song, M. A. Reed, and T. Lee, Adv. Mater. **23**, 1583 (2011).
[3] J. M. Beebe, B. Kim, J. W. Gadzuk, and C. D. Frisbie, J. G. Kushmerick, Phys. Rev. Lett. **97**, 026801 (2006).
[4] J. M. Beebe, B. Kim, C. D. Frisbie, and J. G. Kushmerick, ACS Nano **2**, 827 (2008).
[5] K. Liu, X. Wang, and F. Wang, ACS Nano **2**, 2315 (2008).
[6] A. V. Pakoulev and V. Burtman, J. Phys. Chem. C **113**, 21413 (2009).
[7] G. Wang, T.-W. Kim, G. Jo, and T. Lee, J. Am. Chem. Soc. **131**, 5980 (2009).
[8] H. Song, Y. Kim, Y. H. Jang, H. Jeong, M. A. Reed, and T. Lee, Nature (London) **462**, 1039 (2009).
[9] A. Tan, S. Sadat, and P. Reddy, Appl. Phys. Lett. **96**, 013110 (2010).
[10] G. Noy, A. Ophir, and Y. Selzer, Angew. Chem., Int. Ed. **49**, 5734 (2010).
[11] N. Bennett, G. Xu, L. J. Esdaile, H. L. Anderson, J. E. Macdonald, and M. Elliott, Small **6**, 2604 (2010).
[12] S. H. Choi, C. Risko, M. C. R. Delgado, B. Kim, J.-L. Brédas, and C. D. Frisbie, J. Am. Chem. Soc. **132**, 4358 (2010).
[13] H. Song, Y. Kim, H. Jeong, M. A. Reed, and T. Lee, J. Phys. Chem. C **114**, 20431 (2010).
[14] H. Song, Y. Kim, H. Jeong, M. A. Reed, and T. Lee, J. Appl. Phys. **109**, 102419 (2011).
[15] G. Wang, Y. Kim, S.-I. Na, Y. H. Kahng, J. Ku, S. Park, Y. H. Jang, D.-Y. Kim, and T. Lee, J. Phys. Chem. C **115**, 17979 (2011).
[16] D. Xiang, Y. Zhang, F. Pyatkov, A. Offenhäusser, and D. Mayer, Chem. Commun. **47**, 4760 (2011).
[17] S. Guo, J. Hihath, I. Díez-Pérez, and N. Tao, J. Am. Chem. Soc. **133**, 19189 (2011).
[18] G. Ricoeur, S. Lenfant, D. Guérin, and D. Vuilaume, J. Phys. Chem. C **116**, 20722 (2012).
[19] A. Tan, J. Balachandran, B. D. Dunietz, S. Y. Jang, V. Gavini, and P. Reddy, Appl. Phys. Lett. **101**, 243107 (2012).
[20] S. Guo, G. Zhou, and N. Tao, Nano Lett. **13**, 4326 (2013).
[21] M. L. Trouwborst, C. A. Martin, R. H. M. Smit, C. M. Guédon, T. A. Baart, S. J. van der Molen, and J. M. van Ruitenbeek, Nano Lett. **11**, 614 (2011).
[22] E. H. Huisman, C. M. Guédon, B. J. van Wees, and S. J. van der Molen, Nano Lett. **9**, 3909 (2009).
[23] I. Bâldea, Europhys. Lett. **98**, 17010 (2012).
[24] M. Araidai and M. Tsukada, Phys. Rev. B **81**, 235114 (2010).
[25] Y. Meir and N. S. Wingreen, Phys. Rev. Lett. **68**, 2512 (1992).
[26] P. Hohenberg and W. Kohn, Phys. Rev. **136**, B864 (1964).
[27] W. Kohn and L. J. Sham, Phys. Rev. **140**, A1133 (1965).
[28] Y. Xue, S. Datta, and M. A. Ratner, Chem. Phys. **281**, 151 (2002).
[29] M. Brandbyge, J.-L. Mozos, P. Ordejón, J. Taylor, and K. Stokbro, Phys. Rev. B **65**, 165401 (2002).
[30] J. Zhang, S. Hou, R. Li, Z. Qian, R. Han, Z. Shen, X. Zhao, and Z. Xue, Nanotechnology **16**, 3057 (2005).
[31] R. Li, J. Zhang, S. Hou, Z. Qian, Z. Shen, X. Zhao, and Z. Xue, Chem. Phys. **336**, 127 (2007).
[32] A. R. Rocha, V. M. Garcia-Suarez, S. W. Bailey, C. J. Lambert, J. Ferrer, S. Sanvito, Nat. Mater. **4**, 335 (2005).
[33] A. R. Rocha, V. M. García-Suárez, S. Bailey, C. Lambert, J. Ferrer, and S. Sanvito, Phys. Rev. B **73**, 085414 (2006).
[34] I. Rungger and S. Sanvito, Phys. Rev. B **78**, 035407 (2008).
[35] K. Wu, M. Bai, S. Sanvito, and S. Hou, J. Chem. Phys. **139**, 194703 (2013).
[36] S. Kaneko, T. Nakazumi, and M. Kiguchi, J. Phys. Chem. Lett. **1**, 3520 (2010).
[37] D. den Boer, O. I. Shklyarevskii, M. J. J. Coenen, M. van der Maas, T. P. J. Peters, J. A. A. W. Elemans, and S. Speller, J. Phys. Chem. C **115**, 8295 (2011).
[38] S. V. Aradhya, M. Frei, A. Halbritter, and L. Ventataraman, ACS Nano **7**, 3706 (2013).
[39] T. Kim, H. Vázquez, M. S. Hybertsen, and L. Ventataraman, Nano Lett. **13**, 3358 (2013).

[40]M. Kiguchi, S. Miura, K. Hara, M. Sawamura, and K. Murakoshi, Appl. Phys. Lett. **91**, 053110 (2007).
[41]M. Kiguchi, O. Tal, S. Wohlthat, F. Pauly, M. Krieger, D. Djukic, J. C. Cuevas, and J. M. van Ruitenbeek, Phys. Rev. Lett. **101**, 046801 (2008).
[42]Y. Kim, H. Song, F. Strigl, H.-F. Pernau, T. Lee, and E. Scheer, Phys. Rev. Lett. **106**, 196804 (2011).
[43]F. Prins, A. J. Shaikh, J. H. van Esch, R. Eelkema, and H. S. J. van der Zant, Phys. Chem. Chem. Phys. **13**, 14297 (2011).
[44]M. Bai, J. Liang, L. Xie, S. Sanvito, B. Mao, and S. Hou, J. Chem. Phys. **136**, 104701 (2012).
[45]H. Rong, S. Frey, Y. Yang, M. Zharnikov, M. Buck, M. Wühn, C. Wöll, and G. Helmchen, Langmuir **17**, 1582 (2001).
[46]D. Y. Petrovykh, H. Kimura-Suda, A. Opdahl, L. J. Richter, M. J. Tarlov, and L. J. Whitman, Langmuir **22**, 2578 (2006).
[47]J. M. Soler, E. Artacho, J. D. Gale, A. García, J. Junquera, P. Ordejón, and D. Sánchez-Portal, J. Phys.: Condens. Matter **14**, 2745 (2002).
[48]N. Troullier and J. Martins, Phys. Rev. B **43**, 1993 (1991).
[49]S. García-Gil, A. García, N. Lorente, and P. Ordejón, Phys. Rev. B **79**, 075441 (2009).
[50]K. Wu, M. Bai, S. Sanvito, and S. Hou, Nanotechnology **24**, 025203 (2013).
[51]J. Perdew, K. Burke, and M. Ernzerhof, Phys. Rev. Lett. **77**, 3865 (1996).
[52]H. B. Michaelson, J. Appl. Phys. **48**, 4729 (1977).
[53]See supplementary material at http://dx.doi.org/10.1063/1.4886378 for the bias polarity dependence of the transition voltage of the asymmetric Ag-vacuum-Ag junction, the atomic structure and the equilibrium transmission spectrum of the Pt-vacuum-Pt junction with the two electrode surfaces decorated with a four-atom platinum cluster in the pyramid configuration, eigenchannel analysis the Ag-biphenyl thiol-gold junction in which the phenyl ring is connected to the Au(111) surface directly, the atomic structure and the transport properties of the Pt-biphenyl thiol-Pt junction with the sulfur atom binding at the hollow site of the Pt(111) surface.
[54]D. A. Papaconstantopoulos, *Handbook of the Band Structure of Elemental Solids* (Plenum Press, New York, 1986).
[55]R. Li, S. Hou, J. Zhang, Z. Qian, Z. Shen, and X. Zhao, J. Chem. Phys. **125**, 194113 (2006).
[56]M. Paulsson and M. Brandbyge, Phys. Rev. B **76**, 115117 (2007).